One- and two-photon Absorptions in asymmetrically substituted free-base porphyrins: A density functional theory study

ARTICLE *in* THE JOURNAL OF CHEMICAL PHYSICS · MARCH 2008

Impact Factor: 2.95 · DOI: 10.1063/1.2838776 · Source: PubMed

3 AUTHORS:

Prakash Chandra Jha
KTH Royal Institute of Technology
33 PUBLICATIONS **250** CITATIONS
SEE PROFILE

Boris Minaev
Черкаський національний університ...
321 PUBLICATIONS **3,074** CITATIONS
SEE PROFILE

Hans Agren
KTH Royal Institute of Technology
865 PUBLICATIONS **18,136** CITATIONS
SEE PROFILE

One- and two-photon Absorptions in asymmetrically substituted free-base porphyrins: A density functional theory study

Prakash Chandra Jha,[1,a)] Boris Minaev,[1,2,3] and Hans Ågren[1]
[1]*Theoretical Chemistry, Royal Institute of Technology, AlbaNova, S-106 91 Stockholm, Sweden*
[2]*State University of Technology, 18006 Cherkassy, Ukraine*
[3]*Norwegian University of Science and Technology, 7491 Trondheim, Norway*

(Received 8 January 2007; accepted 8 January 2007; published online 20 February 2008)

Electronic spectra and structures of a new family of free-base porphyrin (H_2P) derivatives with 4-(diphenylamino)stilbene (DPAS) or 4,4′-bis-(diphenylamino)stilbene (BDPAS) asymmetric substituents, recently synthesized and studied by Drobizhev *et al.* [J. Phys. Chem. B **110**, 9802 (2006)] are investigated by density functional theory (DFT) using modern density functionals and the 6-31G* basis set. The time-dependent DFT technique is applied for calculations of one- and two-photon absorption spectra, electric and magnetic dipole moments, and for prediction of electronic circular dichroism for these chiral molecules. The four-band absorption spectrum of the H_2P molecule (Q_x, Q_y, 0-0 and 1-0 bands) is enhanced in single-bond-linked DPAS. This enhancement is explained by hyperconjugation of the almost orthogonal π systems and by small charge-transfer admixtures. The effect is much stronger for the double-bond- and triple-bond-linked DPAS and BDPAS substituents where absorption in the Q region transforms into a two-band spectrum. These molecules with ethenyl and ethynyl bonding of the porphyrin and donor substituent show very strong two-photon absorption in the near-infrared region. DFT calculations explain this by more efficient conjugation between the H_2P and DPAS (BDPAS) chromophores, since they are almost coplanar: "Gerade" states of the H_2P molecule occur in the Soret region and transform into charge-transfer states with nonzero transition moments. They are responsible for the strong two-photon absorption effects. Mixing of excitations in both chromophores explains the broadening of the Soret band. Though the calculated two-photon absorption cross sections are overestimated, the qualitative trends are reproduced and help understanding the whole genesis of spectra of these asymmetrically substituted H_2P derivatives. © *2008 American Institute of Physics*.
[DOI: 10.1063/1.2838776]

I. INTRODUCTION

Porphyrins are widely spread in living matter, they occur in green plants (chlorophyll), in blood vessels (hemoglobin), and in numerous cytochromes, to mention a few of many examples.[1,2] The importance of porphyrin pigments in photobiology (photosynthesis, photodynamic therapy, and light treatment for blood transfusion) has led to a vast body of spectroscopic studies.[2–6] By these reasons porphyrins have been labeled the "pigments of life."[8] New synthetic porphyrins have also been ascribed much attention.[3,7,9–11] Much of this work has recently been focused on porphyrin assemblies for light-harvesting purposes, porphyrin dendrimers and dimers containing mimics of the photosynthetic reaction center,[9,10] nonlinear optics,[7,12] and electronic devices.[13–16] The last decade has witnessed an explosion of experimental studies of new synthetic porphyrins which have yielded very useful information about their electronic structures and optical spectra (see, for example, Refs. 2 and 17–19), but it has not always been possible to provide a well reasoned explanation of the results obtained.[12,20–24]

A new family of free-base porphyrin derivatives with asymmetric substitution at the mesoposition by 4-(diphenylamino)stilbene (DPAS) or 4,4′-bis-(diphenylamino)stilbene (BDPAS) substituents from one side and by dichlorophenyl from the other side (Fig. 1) has recently been synthesized and studied by optical spectroscopy.[7] Drobizhev *et al.* have measured one-photon (1PA) and two-photon (2PA) absorption and fluorescence spectra; they have obtained systematic shifts and enhancement of 1PA spectra both in the Q and Soret band regions. This means that the main chromophore is still the porphyrin part of the molecules. Also, as much as two order of magnitude increase of the 2PA cross section in the Soret band region (excitation wavelength around 800 nm) has been obtained.[7]

This new family of porphyrins exhibits interesting features which have been interpreted on pure empirical grounds in terms of polarization and solvent effects.[7] Proper understanding based on *ab initio* calculations of these optical phenomena is important for a complete theory of porphyrin chromophores. Although the absorption and emission spectra of many porphyrins are well known since a long time,[4,25] some spectroscopic features such as magneto-optical phenomena,[2] vibronic band structure of fluorescence and phosphorescence spectra,[6,26–29] and Raman spectra from ex-

[a)]Electronic mail: prakash@theochem.kth.se.

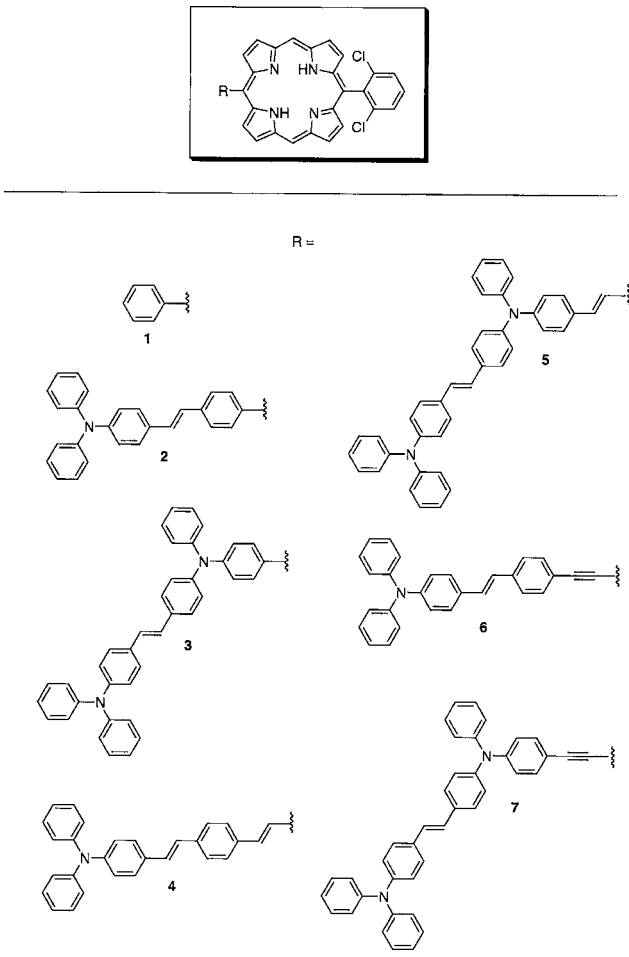

FIG. 1. Studied molecules.

cited states,[18,30] two-photon spectroscopy,[12] etc., are not completely understood so far.

Free-base porphyrin (H_2P) is the basic building block and the electronic "heart" of porphyrins. The excited electronic states of H_2P have long been of theoretical interest as a testing ground of quantum chemistry applications in molecules with a high symmetry.[4,20,22,23,31–34] Some new explanations for the free-base porphyrin spectroscopy has recently been obtained on the basis of rigorous theoretical investigations.[35–38] The electronic absorption spectra of the H_2P molecule in the visible region consists of four weak bands usually called the Q^{I}–Q^{IV} bands.[4,25,39] In the UV region there is a very strong Soret band (or B band) and three other bands (N, L, and M) of weaker intensity.[4] The interpretation of the H_2P spectra is based on the useful four orbital model of Gouterman which considers the two highest occupied (b_1,b_2) and two lowest unoccupied (c_1,c_2) molecular orbitals (MO).[31] In the idealized D_{4h} point group, these MOs have symmetry a_{2u}, a_{1u}, and e_g, respectively.[31] The single-electron excitations $b_1 \rightarrow c_1$ and $b_2 \rightarrow c_2$ are mixed by configuration interaction (CI) and provides Q_x and B_x transitions; the former is forbidden by quenching of two equal transition moments, the latter is very intense since the transition moments are added. A similar situation occurs for the Q_y and B_y transitions produced by CI mixing of the $b_1 \rightarrow c_2$ and $b_2 \rightarrow c_1$ single-electron excitations. For metal porphyrins

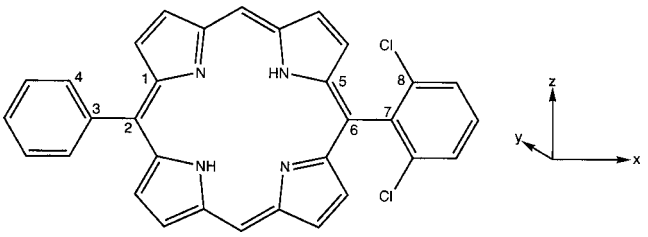

FIG. 2. Figure showing the dihedral angle labeling and the selection of axis.

which possess a very high D_{4h} symmetry, each pair of states are degenerate. In fact, free-base porphyrin belongs to the lower symmetry of the D_{2h} point group and the former degenerate e_g orbitals are now split into $b_{2g}(c_2)$ and $b_{3g}(c_1)$ MOs. The two highest occupied (b_1,b_2) orbitals are very close in energy and have a_u and b_{1u} symmetries, respectively. Here, the choice of axes is the same as that in Gouterman's paper:[31] the N–H bonds are along the x axis, while the z axis is perpendicular to the molecular plane.

The simple four orbital model of Gouterman has been supported by calculations with time-dependent density functional theory (TD DFT).[33,34,37,40] Similar results have been obtained in a number of recent TD DFT calculations.[22,23,34,42] In all these and previous studies,[4,20,32,33,43] the Q^{I} and Q^{III} bands (at 1.98 and 2.42 eV) (Ref. 39) are interpreted as vertical transitions from the ground state to the $1\,^1B_{3u}$ and $1\,^1B_{2u}$ states, respectively. The tentative proposal that these vertical transitions coincide with the 0-0 bands has been widely accepted.[4,20,31–34] The more intense bands, Q^{II} and Q^{IV}, were proposed to correspond to 0-1 transitions on the basis of the relative constancy of their spacing from the electronic origin, as the latter is shifted by substituents in a large number of porphyrins.[4] Vibronic bands in H_2P absorption and emission spectra associated with a change both in electronic and vibrational states have been considered by Perrin *et al.*[44] and in a recent DFT study with more realistic vibrational modes and force fields.[37] We will use these data for assignment of the Q^{II} and Q^{IV} absorption bands in the porphyrin derivatives.

II. METHOD OF CALCULATIONS

The studied molecules are presented in Fig. 1. These are 4-(diphenylamino)stilbene (DPAS) (molecules **2, 4**, and **6**) and 4,4′-bis-(diphenylamino)stilbene (BDPAS) (molecules **3, 5**, and **7**) attached at the mesoposition to free-base porphyrin; at the opposite mesoposition, the 2,6-dichlorophenyl substituent is attached. The simplest molecule (**1**) contains a phenyl substituent instead of DPAS. Numeration of atoms and choice of axes for the molecules are shown in Fig. 2. Becke's three-parameter hybrid functional[41] (B3LYP) and 6-31G* basis set[45,46] are used for geometry optimization and TD DFT calculations are carried out for one-photon absorption. The geometries of all molecules are optimized for the singlet ground state (S_0) and the vertical excitation energies to the six lowest singlet excited states with the $S_0 \rightarrow S_n$ transition intensities obtained with the GAUSSIAN 03 code.[47] Excited states wave functions extracted from the TD DFT calculations are analyzed in terms of an expansion of single-

electron excitations taking into account the largest coefficients. Rotational strength of electronic circular dichroism is calculated using gauge-invariant atomic orbitals in the velocity formulation according to Ref. 48.

The two-photon transition matrix element S_{ab} can be identified from the sum-over-states formula and can be written as

$$S_{ab} = \sum_i \left[\frac{\langle o|\mu_a|i\rangle\langle i|\mu_b|f\rangle}{\omega_i - \omega_f/2} + \frac{\langle o|\mu_b|i\rangle\langle i|\mu_a|f\rangle}{\omega_i - \omega_f/2} \right], \quad (1)$$

where the summation includes all the intermediate states, including the ground state and final state. In Eq. (1), ω_i denotes the excitation energy of the intermediate state $|i\rangle$, ω_f denotes the excitation energy of the final state $|f\rangle$, and μ_a and μ_b are the electric dipole operators. The total 2PA probability δ_{TP} for a molecule in gas phase or in solution can subsequently be obtained by applying orientational averaging according to McClain[49] as

$$\delta_{TP} = F\delta_F + G\delta_G + H\delta_H, \quad (2)$$

where the definition of F, G, and H follows from McClain's work;[49] the value for each of these parameters is equal to 2 for linearly polarized light. Since, we are interested to compare the theoretically calculated 2PA cross sections with the experimentally reported ones in cm^4 s $photon^{-1}$, we need to relate the macroscopic cross section with the transition probability. This relationship is given by

$$\sigma_{2PA} = \frac{4\pi^2 \alpha a_0^5 \omega^2 g(\omega)}{15c} \delta_{TP}, \quad (3)$$

where α is the fine structure constant, ω is a transition frequency, $g(\omega)$ provides the spectral line profile, and c is the velocity of light in vacuum. At this point, it is important to mention that the assumptions made about the band shape function leads to increase in the uncertainty associated with σ_{2PA} calculation. It is important to mention here that some earlier investigators have used a variant of Eq. (3), in which $g(\omega)$ is divided by a damping factor Γ that reflects the lifetime broadening of the final state in the transition.[50–52] No doubt, both $g(\omega)$ and Γ will vary from one molecule to another and depends on a number of variables including vibronic structure, solvent, and temperature. However, over a period of time, it has become a common practice to replicate similar values of $g(\omega)$ and Γ from one system to the another. The only way to minimize this uncertainty is to incorporate the molecule dependent parameters into $g(\omega)$. No doubt, each transition will have a unique line shape function which will be very complicated in those instances where vibronic structure cannot be resolved. In our case, we will represent the line shape function for all the molecules as a Gaussian profile centered at the calculated energy maxima of the final state as[53]

$$g(\omega) = g_{max} \exp\left(\frac{-4\ln 2}{(\Delta\omega)^2} (2\omega - \omega_f)^2 \right), \quad (4)$$

where $\Delta\omega$ is the full width at half maximum of the given band. Since, $g(\omega)$ is normalized in frequency space,

$$g_{max} = \left(\frac{4\ln 2}{\pi\Delta\omega^2} \right)^{1/2} = \frac{0.939}{\Delta\omega}. \quad (5)$$

Consequently, for a given two-photon absorption bandwidth, the maximum of $g(\omega)$ will equal g_{max}. Since, all the molecule studied in this work can be considered as the derivatives of free-base porphyrin and we will be discussing all our results with respect to it, hence, we have taken ω=0.26 eV.[53] At this point it is necessary to mention that the limitation of conventional TD DFT in treatments of conjugated systems with charge-transfer (CT) character, TD DFT methods can fail sometime. In fact, recently, it has been shown[54–57] that most functionals fail in predicting the properties of charge-transfer processes. To overcome these difficulties, new hybrid functionals called CAMB3LYP,[58] which combine properties of B3LYP and the long range corrections for exchange potential, have been developed. In fact, recently, it has been shown that with this functional one can expect to get reliable two-photon results compared to even highly correlated coupled cluster response calculations.[59,60] Keeping these points in mind we will compare our two-photon absorption results with both the functionals. All two-photon calculations presented here are performed with the B3LYP as well as CAMB3LYP functional using a new version of the DALTON code.[61]

III. RESULTS AND DISCUSSION

Results of the present B3LYP/6-31G* calculations of the six low-lying singlet excited states and the corresponding singlet-singlet one-photon absorption spectra of asymmetrically substituted free-base porphyrin (molecules **1, 2, 4**, and **6** in Fig. 1) are presented in Tables II–V. Results for the other molecules in Fig. 1 are discussed in the text as they belong to the same class of molecules.

Geometry optimization indicates that the mutual orientation of the porphyrin ring and the substituents changes along the series of the studied molecules. In molecule **1**, the porphyrin ring is almost orthogonal to both substituents [the dihedral angle C(1)-C(2)-C(3)-C(4) is equal to 64.00°; the dihedral angle from the opposite side C(5)-C(6)-C(7)-C(8) is equal to 89.94°, Fig. 2]. The dichlorophenyl ring remains practically orthogonal in all molecules, but the DPAS (and BDPAS) substituents becomes coplanar with the increase of the conjugation length. The corresponding dihedral angle diminishes to 60.40°, 41.62°, 36.87°, and 3.25° in molecules **2, 4, 5**, and **6**, respectively, while in molecule **7** it is equal to 4.82°. This means that the nearest phenyl ring connected by the triple bond with the H_2P part is almost coplanar with the porphyrin moiety. These structural changes influence the degree of conjugation as well as hyperconjugation and will thus provide essential effects on the spectral properties. First, we need to compare the parent molecule **1** of the present series with the main building block, free-base porphyrin. We have also calculated a single-substituted molecule with R=H (Fig. 1). Comparison between calculated spectra of free-base porphyrin and this asymmetric molecule indicates a small redshift (5.4 nm) and enhancement of the Q_x band; the oscillator strength for this new molecule (R=H) is still rather weak (f=0.002). We have to stress that the transition energy of the

Q_x band is overestimated in all TD DFT calculations with different functionals while the Q_y band is in better agreement with observations.[23,34,56] At the same time, *ab initio* methods, like CASPT2,[56,62] SAC-CI,[63] and MRMP,[64] strongly underestimate the Q_x-band transition energy. Thus, in spite of some small errors, the TD DFT approach seems to be the best method to treat porphyrins, especially with large asymmetric substituents.

All other $\pi\pi^*$ bands in the single-substituted molecule with R=H have similar redshifts of the order of 5–3 nm. The Q_y band is more enhanced (f=0.003). Transitions to the Soret states have oscillator strengths equal to 0.461 and 0.729 for the $2\,^1B_{3u}$ and $2\,^1B_{2u}$ analogs, respectively. Thus, we predict an increase of the absorption intensity of the main porphyrin bands upon the asymmetric substitution (R=H). The most important prediction is obtained for the former forbidden transitions to the "gerade" states, $1\,^1B_{1g}$ and $2\,^1A_g$; they become electric dipole allowed and get oscillator strengths equal to 0.018 and 0.009, respectively.

There are two states at higher energy (above 3.8 eV), which are of $3\,^1B_{2u}$ and $3\,^1B_{3u}$ type. They have larger oscillator strengths (0.51 and 0.78, respectively) and higher contributions of excitations from the $4b_{1u}$ orbital, which is not present in the Gouterman model. We cannot see any reasons to consider these states as the exclusive representatives of the Soret band, as has been proposed in some papers,[55,56] where the $2\,^1B_{3u}$ and $2\,^1B_{2u}$ terms have been assigned to the N bands. The N bands are very weak;[4] they probably are connected with the "gerade" state being induced by vibronic perturbations. Also, since TD DFT calculations are very time consuming for system as large as the ones presented in this paper, we restrict our study to the treatment of the six lowest excited states. Thus, we exclude analogies of the $3\,^1B_{2u}$ and $3\,^1B_{3u}$ states and $n\pi^*$ transitions, which are above 3.8 eV and have not been recorded in experimental work.[7]

Keeping the above mentioned facts into consideration, we can start to compare H_2P with the parent molecule **1** of the present series. As follows from Table II, the Q and B states are presented by mixture of four main configurations (transitions between all four molecular orbitals of the Gouterman model). Since the choice of axes is not conventional for asymmetrically substituted molecules; we choose the x axis as the long axis of the species, thus the former x and y axes are rotated by 45°. Since the porphyrin ring is almost planar in all optimized molecular structures, the z axis is determined as being perpendicular to this plane. Thus, Table II indicates that both Q bands in molecule **1** change their polarization corresponding to the new "long" axis (x) of the system; at the same time their intensity is strongly enhanced in comparison with the H_2P molecule.

The intensity ratio of the $Q_x(0,0)$ and $Q_x(1,0)$ band in the parent molecule **1** and in free-base porphyrin is quite different. The vibronic band is stronger in the former molecule. The phenyl rings attached at two opposite mesopositions provide definite changes in the calculated IR and Raman spectra of the H_2P molecule. A reduction of symmetry removes the "gerade" and "ungerade" classification and provides some mixing of free-base porphyrin modes with phenyl vibrations.

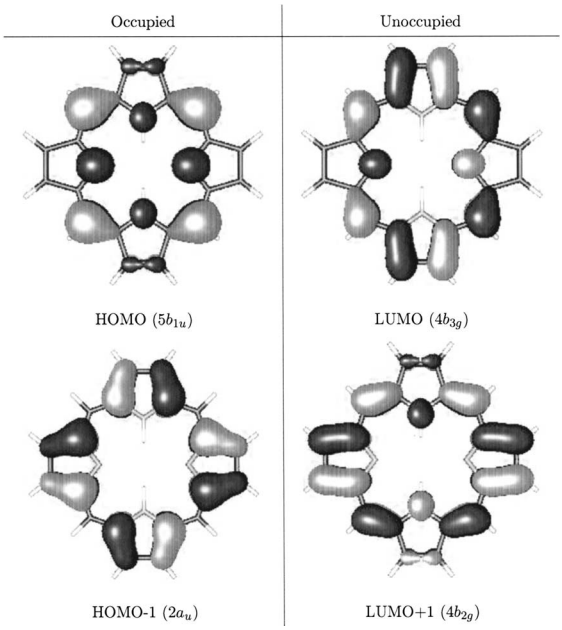

FIG. 3. Four orbitals of free-base porphyrin, obtained by B3LYP/6-31G* method.

From vibronic DFT calculations,[37] it follows that the maximum of the 1-0 band in free-base porphyrin absorption at 556 nm is mostly connected with the fundamental mode $\nu_{10}(a_g)$=1610 cm^{-1} (in classification of Li and Zgierski[65]). This is the asymmetric C_α-C_m stretch motion of the methine bridges. Asymmetric substitutions at the meso-C_m positions strongly influence this vibration; it is mixed with the C=C vibrations of the phenyl rings and becomes more active in intensity borrowing for the M_x transition moment. This leads to an enhancement of the vibronic perturbation and to more intense 1-0 transitions in the Q_x bands.

Comparison of the single-substituted molecule (R=H, Fig. 1) with molecule **1** indicates that the $Q_x(0,0)$ band is further redshifted by 8.4 nm and enhanced (from f=0.002 to f=0.009). The $Q_y(0,0)$ band is also redshifted (by 8.8 nm) and its oscillator strength increases from f=0.003 to f=0.018. The substituents produce a strong polarization effect. One should recall that both Q bands are polarized along the x (long) axis (Table II); this means that the orbital nature of these optical excitations in the visible region is changed. In fact, the highest occupied molecular orbital (HOMO) (MO 137) and lowest unoccupied molecular orbital (LUMO) (MO 138) represent mostly the $5b_{1u}$ and $4b_{2g}$ orbitals, respectively, with appreciable contributions from the phenyl substituent (about 9%) and even from the dichlorophenyl moiety (3%). Orbitals with numbers 136 and 139 represent almost pure $2a_u$ and $4b_{3g}$ MOs, respectively. Thus, the first two excited states in Table II correspond to the Q bands of H_2P with small admixture of charge-transfer contributions which are partly presented in configurations (137→139) and (136→138). They actually provide charge transfer in the opposite directions. The two Q states have different phases of these charge-transfer contributions (Table II).

The Soret band of free-base porphyrin consists of two close-lying transitions (see Fig. 3). Their wave functions are determined by the same configurations such as those for the

TABLE I. Electronic absorption spectrum of free-base porphyrin. ΔE is an excitation energy (eV), f is an oscillator strength, and M_a is a projection of the electric dipole transition moment (a.u.) on the a axis.

State D_{2h}	Main CI contributions	ΔE Calc.	ΔE Expt.	M_a $\lvert M\rvert$	M_a a	f Calc.	f Expt.
$1\,^1B_{3u}$	$0.48(2a_u\rightarrow 4b_{3g})+0.56(5b_{1u}\rightarrow 4b_{2g})$	2.28	1.98	0.020	x	0.0001	0.01
$1\,^1B_{2u}$	$-0.47(2a_u\rightarrow 4b_{2g})+0.52(5b_{1u}\rightarrow 4b_{3g})$	2.44	2.42	0.025	y	0.0001	0.06
$2\,^1B_{3u}$	$0.45(4b_{1u}\rightarrow 4b_{2g})-0.37(2a_u\rightarrow 4b_{3g})+0.20(5b_{1u}\rightarrow 4b_{2g})$	3.33	3.33	2.26	x	0.42	1.15
$2\,^1B_{2u}$	$0.37(4b_{1u}\rightarrow 4b_{3g})+0.35(2a_u\rightarrow 4b_{2g})+0.31(5b_{1u}\rightarrow 4b_{3g})$	3.51	3.33	2.704	y	0.63	1.15
$1\,^1B_{1g}$	$0.68(3b_{3g}\rightarrow 4b_{2g})$	3.42[b]	⋯	0		0	⋯
$2\,^1A_g$	$0.68(3b_{2g}\rightarrow 4b_{3g})$	3.61	⋯	0		0	⋯

[a]Reference 25.
[b]Excitation to the $1\,^1B_{1g}$ state is characterized by a big magnetic dipole transition moment (1.77β, where β is Bohr magneton).

Q_x and Q_y states, but these are connected by the opposite signs in the Q states of H_2P; the transition moments are almost canceled. The narrow width of the Soret band is probably determined by vibronic mixing of the $2\,^1B_{3u}$ and $2\,^1B_{2u}$ states induced by b_{1g} in-plane vibrations.[37] It follows from our calculations that the total oscillator strength of the Soret band of free-base porphyrin increases upon substitution in molecule **1** from 1.19 to 1.56; such an enhancement agrees with the experimental extinction coefficient measurements.[4,7]

The Soret band also includes contributions from the $4b_{1u}\rightarrow 4b_{2,3g}$ excitations (Table I and II). Molecular orbital 134 of molecule **1** is an analog of the $4b_{1u}$ orbital of H_2P. It is localized on the nonprotonated pyrrole rings and has an appreciable π contribution (16%) of the phenyl substituent. This provides an additional increase of CT character (from the substituent to porphyrin ring) for the Soret band in molecule **1**. The former "gerade" states (S_4 and S_6 in Table II) are further redshifted by 2–3 nm, but the corresponding absorption is not as strong as in the molecule with one substituent (R=H in Fig. 1). Especially, the transition to the S_4 state is less enhanced (f=0.001 in comparison with f=0.0018 for R=H). This enhancement of the former forbidden transition strongly depends on the asymmetry of substitution.

A. Single-bond-linked molecules 2 and 3

The increase of π delocalization in the left substituent by the diphenylamino-stilbene attachment (compare molecules **1** and **2** in Tables II and III, respectively) provides further shift and enhancement of the Q bands and the Soret band broadening in agreement with experimental spectra.[7] The calculated redshifts of the Q_x and Q_y (0-0) peaks are equal to 10.8 and 22.8 nm, respectively. The corresponding experimental shifts are equal to 10 and 25 nm, respectively,[7] which makes credit to our DFT approach. The intensity enhancement of both Q (0-0) transitions is quite big; calculations predict more than an order of magnitude increase of the oscillator strength in a very reasonable agreement with the experimental spectra.[7] Again, the intensity of the Q_y band is almost twice as large in comparison with the Q_x band (Tables II and III) in accord with the measured extinction coefficients.[7] The notation Q_y is used here to stress the ge-

TABLE II. Electronic absorption spectrum of free-base porphyrin derivative **1**. ΔE is an excitation energy (eV), f is an oscillator strength, and M_a is a projection of the electric dipole transition moment (a.u.) on the a axis. Rotatory strength (R) of electronic circular dichroism (ECD) in 10^{-10} erg esu cm/G.

State D_{2h}	Main CI contributions	ΔE Calc.	ΔE Expt.[a]	M_a M	M_a a	f Calc.	f Expt.[a]	ECD R
S_1Q	$0.42(137\rightarrow 139)-0.37(136\rightarrow 138)$	2.22	2.21	0.41	x	0.009	≈0.01	0.18
	$+0.35(137\rightarrow 138)+0.28(136\rightarrow 139)$			0.02	y			
S_2Q	$-0.32(137\rightarrow 139)+0.31(136\rightarrow 138)$	2.37	2.33	0.56	x	0.018	≈0.04	0.18
	$+0.42(137\rightarrow 138)+0.35(136\rightarrow 139)$			0.06	y			
S_3B	$0.20(137\rightarrow 139)+0.27(136\rightarrow 138)$	3.25	3.06	2.26	x	0.604	≈0.8	−3.95
	$+0.16(137\rightarrow 138)-0.27(136\rightarrow 139)$			1.57	y			
	$0.28(134\rightarrow 138)+0.27(134\rightarrow 139)$			−0.06	z			
$S_4\pi\pi^*$	$0.54(135\rightarrow 138)+0.41(135\rightarrow 139)$	3.35	⋯	0.095	x	0.001	⋯	−1.26
S_5B	$0.24(137\rightarrow 139)+0.27(136\rightarrow 138)$	3.39	3.06	2.67	x	0.96	≈0.8	−2.80
	$-0.21(137\rightarrow 138)+0.29(136\rightarrow 139)$			2.09	y			
	$-0.20(134\rightarrow 138)+0.15(134\rightarrow 139)$			−0.07	z			
$S_6\pi\pi^*$	$-0.41(135\rightarrow 138)+0.54(135\rightarrow 139)$	3.56	⋯	0.023	x	0.007	⋯	0.43

[a]Reference 7.

TABLE III. Electronic absorption spectrum of free-base porphyrin derivative **2**. ΔE is an excitation energy (eV), f is an oscillator strength, and M_a is a projection of the electric dipole transition moment (a.u.) on the a axis. Rotatory strength (R) of electronic circular dichroism (ECD) in 10^{-10} erg esu cm/G.

State D_{2h}	Main CI contributions	ΔE Calc.	ΔE Expt.[a]	M_a M	M_a a	f Calc.	f Expt.[a]	ECD R
S_1Q	0.37(208→209)−0.27(207→210)	2.18	1.94	−1.49	x	0.118	≈0.1	2.44
	−0.27(208→210)+0.26(207→209)			0.03	y			
	−0.30(206→209)−0.27(206→210)			−0.01	z			
S_2Q	0.49(208→209)+0.23(207→210)	2.28	2.38	−1.90	x	0.201	≈0.2	−2.2
	+0.30(208→210)+0.08(207→209)			−0.00	y			
	0.30(206→209)−0.14(206→210)			−0.02	z			
S_3	−0.31(208→209)+0.05(207→210)	2.42		0.75	x	0.034		3.1
	+0.22(208→210)+0.50(207→209)			−0.02	y			
	0.10(206→209)−0.31(206→210)			−0.02	z			
S_4	−0.04(208→209)−0.41(207→210)	2.50		0.00	x	0.004		0.4
	+0.51(208→210)+0.11(207→209)			−0.25	y			
	0.21(206→209)−0.01(206→210)			−0.02	z			
S_5B	0.59(208→211)+0.05(207→210)	3.02	2.93	5.40	x	2.154	≈2	91.6
	−0.15(207→209)			−0.09	y			
	−0.24(206→210)			−0.04	z			
S_6	−0.24(208→211)+0.17(207→210)	3.22	3.34	0.65	x	0.157	≈0.3	22.8
	+0.40(205→209)−0.14(207→209)			−1.25	y			
	−0.21(206→209)−0.20(206→210)			−0.07	z			

[a]Reference 7.

neric connection with the pure porphyrin spectrum; in fact, both the Q_x and Q_y bands are predominantly polarized along the x axis (Table III).

The Soret band itself (transition to the S_5 state, Table III) has a large contribution of the (208→211) configuration which corresponds to porphyrin excitation with a significant admixture of CT from the porphyrin ring (and diphenylamin) to the stilbene fragment. The HOMO 208 of molecule **2** describes a strongly delocalized electron with large density on the diphenylamine group [Fig. 4(a)]; at the same time, the orbital 208 corresponds to the $5b_{1u}$ HOMO of the free-base porphyrin ring [Fig. 4(b)]. This is an interesting example of hyperconjugation between two noncoplanar chromophores. The MO 211 is predominantly concentrated at the stilbene moiety though it is also delocalized into the porphyrin ring [Fig. 4(c)]. Thus, the (208→211) configuration describes excitations in both chromophores. This significant change of the orbital nature of the excited state explains the enhancement and also the redshift of the Soret band (Table III).

The broadening of the Soret band has been tentatively explained by a partial overlap with a substituent absorption.[7] This corresponds to our previous analysis with additional account of a new state S_6. Indeed, the state S_6 (Table III) includes a large contribution of the (205→209) excitation. MO 205 is mostly localized at the substituent, while the LUMO (209) is distributed in the porphyrin ring with small admixtures from the stilbene fragment. Thus, the occurrence of a new state S_6 with moderate transition intensity can be explained by a local excitation in the substituent with some charge-transfer character.

Our results for molecules **3** and **2** are quite similar, which is in agreement with experiment.[7] Thus, we omit the corresponding discussion of molecule **3** and only note that a small redshift (about 2 nm) for the Q bands of molecule **3** is predicted by our calculations in agreement with experimental data.[7]

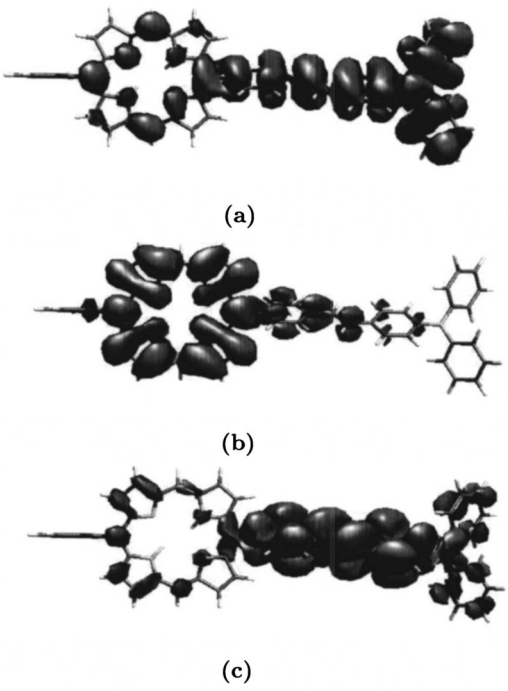

FIG. 4. (a) HOMO (208) of molecule **2**. (b) LUMO (209) of molecule **2**. (c) MO 211 of molecule **2**.

TABLE IV. Electronic absorption spectrum of free-base porphyrin derivative **4**. ΔE is an excitation energy (eV), f is an oscillator strength, and M_a is a projection of the electric dipole transition moment (a.u.) on the a axis. Rotatory strength (R) of electronic circular dichroism (ECD) in 10^{-10} erg esu cm/G.

State D_{2h}	Main CI contributions	ΔE Calc.	ΔE Expt.[a]	M_a M	M_a a	f Calc.	f Expt.[a]	ECD R
S_1X	0.56(215→216)−0.22(213→217)	2.05	2.10	3.70	x	0.694	≈0.4	−20.3
	−0.11(214→216)−0.13(214→217)			0.42	y			
	+0.22(215→217)+0.20(213→216)			−0.24	z			
S_2Q	−0.31(215→216)−0.22(213→217)	2.14	1.91	2.32	x	0.283	≈0.25	−23.1
	−0.03(214→216)−0.01(214→217)			0.02	y			
	+0.44(215→217)+0.38(213→216)			0.03	z			
S_3	0.16(215→216)+0.30(213→217)	2.34	2.38	0.41	x	0.010	≈0.04	−23.1
	−0.07(214→216)+0.05(214→217)			−0.01	y			
	+0.15(215→217)+0.59(213→216)			−0.07	z			
S_4	0.02(215→216)+0.03(213→217)	2.50	2.45	−0.10	x	0.012	≈0.05	−23.1
	−0.07(214→216)+0.49(214→217)			0.41	y			
	+0.43(215→217)−0.24(213→216)			0.12	z			
S_5B	0.57(215→218)−0.30(213→217)	2.83	2.85	−5.39	x	2.013	≈2.0	35.0
	+0.14(214→216)+0.08(214→217)			0.01	y			
	+0.15(215→217)+0.07(213→216)			0.04	z			
S_6	0.60(212→216)−0.17(213→217)	2.99	3	−1.21	x	0.118	≈0.2	−27.2
	+0.14(214→216)+0.10(214→218)			−0.33	y			
	−0.22(215→218)+0.01(213→216)			−0.18	z			

[a]Reference 7.

B. The role of "gerade" states

Besides the well-known characteristic absorption of the free-base porphyrin chromophore in molecules **1** and **2**, there are very weak $\pi\pi^*$ transitions which were strictly forbidden in the H_2P molecule by symmetry; these are transitions to the $1\ ^1B_{1g}$ and $2\ ^1A_g$ states (Table I). The role of these states has been discussed recently[12] in connection with 2PA of free-base tetraphenylporphyrin (H_2TPP). The "gerade" states are forbidden for one-photon transitions but they become allowed for 2PA. An intense 2PA has been detected in the region of the Soret band in tetraphenyl porphyrin (H_2TPP).[12] Transitions to the $1\ ^1B_{1g}$ and $2\ ^1A_g$ states become visible in dendrimers of H_2TPP and ZnTPP with large substituents in the mesoposition.[66]

In the asymmetric molecules **1–7**, where the center of inversion is removed and the porphyrin chromophore is conjugated with the (diphenylamino)stilbene fragments by strong involvement of CT excitations, the "gerade" states are also accessible by one-photon absorption. These are the S_4 and S_6 states in molecule **1** (Table II) and S_3, S_4 states in molecule **2** (Table III), discussed so far. Prolongation of the conjugation chain in molecule **2** provides enhancement of one-photon absorption to the S_3 state with long axis (x) polarization. We shall return to the discussion of the "gerade" states later on in connection with calculations of 2PA.

C. Double-bond (ethenyl)-linked molecules 4 and 5

In the ethenyl-linked molecules a dramatic change occurs in the former Q-band absorption region, 530–670 nm,[7] in comparison with the molecules **1–3**. Instead of four characteristic Q bands of the free-base porphyrin chromophore, a much more intense new band occurs at 590 nm and the former Q^I band is redshifted and enhanced. Our DFT calculations also predict a dramatic change in this spectral region (Table IV). A new intense transition is calculated at 2.05 eV which we interpret as a new intense band observed at 2.10 eV (590 nm). We shall call it the "X band," since it has large electric dipole transition moment along the x axis. Since the TD DFT/B3LYP method systematically overestimates the energy of the Q_x transition,[22,36] the new X state becomes lower in energy than the Q_x state (Table IV). One cannot be confused because of this artifact of the TD DFT/B3LYP method as it is very obvious. The first absorption band at 675 nm represents a transition to the Q_x state, which occurs as the second S_2 state in our calculation (Table IV). Its intensity is also enhanced in agreement with observations.[7]

The strong new X band at 590 nm is determined mostly by a HOMO-LUMO excitation [configuration (215→216) in Table IV]. Molecular orbital 215 includes the porphyrin $5b_{1u}$ orbital (30%) and the whole substituent even with contributions from the terminal diphenylamin group [Fig. 5(a)]. Molecular orbital 216 includes 90% of porphyrin of the $4b_{3g}$ orbital with small contributions from the nearest ethenylbenzene group [Fig. 5(b)]. Thus, the new band represents a local excitation in porphyrin with large admixture of CT transition from far-remote nitrogen of the terminal diphenylamin group to the porphyrin ring. The Q_x band at 675 nm has a similar configuration expansion but consists of rather different coefficients (S_2 state in Table IV) and includes the CT character to a less extend. Two weak transitions to the states S_3, S_4 (Table IV) are seen in the absorption spectrum

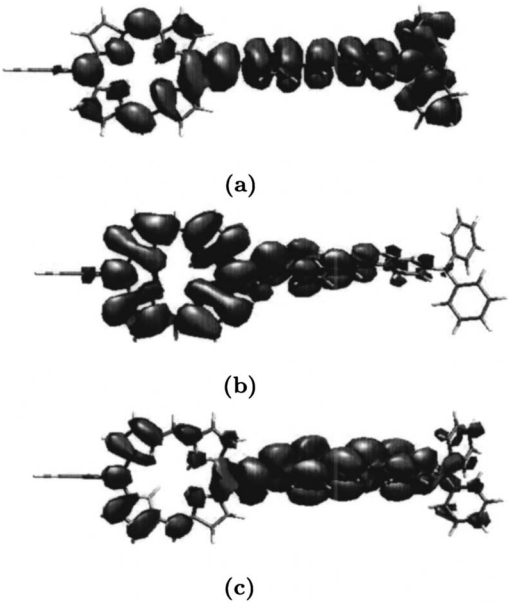

FIG. 5. (a) HOMO (215) of molecule **4**. (b) LUMO (216) of molecule **4**. (c) MO 218 of molecule **4**.

of molecule **4** as a clear shoulder at 540 nm.[7] They are mostly of CT nature. The Soret band indicates a very strong broadening and a redshift of the band maximum to 430 nm.[7] We can relate this redshift to a stronger conjugation between free-base porphyrin and the ethenyl-bound substituent. The S_5 state (Table IV) has a large contribution of the configuration 215→218, and MO 218 includes both porphyrin and stilbene fragments [the latter is much more present, Fig. 5(c)]. In molecule **4**, both chromophores are more coplanar than in molecules **1–3** and the ethenyl link provides more conjugation. Excitation 215→218 creates a transition moment (long axis) with destructive contributions from both chromophores. Thus, the intensity of the Soret band in molecule **4** is slightly lower than in molecules **2** and **3**.

Similar results have been obtained for the other double-bond (ethenyl)-linked molecule **5**. The new intense *X* band is predicted to be redshifted by 13.3 nm in comparison with molecule **4**, which is in a good agreement with experimental data (12 nm).[7] This transition has a larger contribution from the HOMO-LUMO excitation: 0.63 (259→260). Thus, it includes more CT character from the far-remote nitrogen atom to the porphyrin ring.

The *Q*-band in molecule **5** is less shifted in comparison with molecule **4** in our calculation (7.7 nm) which agrees with the experimental shift (7 nm).[7] The highest energy calculated transition in molecule **5** is a weak CT transition at 2.9 eV (S_6). Since we have calculated only six excited states in each molecule, the Soret transition is not present in this calculation. It means that the Soret state in molecule **5** would be higher than at least 2.9 eV. This result does not contradict the experimental measurements,[7] where the Soret state in molecule **5** is detected at 2.92 eV, thus indicating a big blueshift (9 nm) in comparison with molecule **4**.

D. Triple-bond (ethynyl)-linked molecules 6 and 7

The triple bond provides more possibility for hyperconjugation with the porphyrin ring, since it possesses two mutually orthogonal π_y and π_z systems. The former would be conjugated with the phenyl ring and the latter would be conjugated with the porphyrin π_z system, if the planes of both chromophores are orthogonal. Because of this sensitivity to hyperconjugation, the two chromophores are almost coplanar at the optimized geometry of molecule **6**. In the ethynyl-linked DPAS molecule (**6**) the same two-band structure in the *Q* region remains as in molecules **4** and **5**. It is interesting to compare the ethenyl-linked and ethynyl-linked DPAS molecules (**4** and **6**). As follows from our calculation (Table V), the intense *X* band is enhanced and redshifted in comparison with the ethenyl-linked molecule **4** in complete agreement with the experimental spectra.[7] The transition energy of the first observed Q_x band is overestimated in the DFT calculations, as usual, and provides the second S_2 state in Table V. The new *X* band corresponds to the HOMO→LUMO excitation with a larger expansion coefficient than in molecule **4** [Figs. 6(a) and 6(b)]. The orbital nature of the *X* excited state is similar in both molecules with more pronounced CT character in molecule **6**. Charge transfer from the DPAS substituent to the porphyrin ring is dominating, though the local excitations in the porphyrin ring is also present.

We get further intensity increase of the Soret band in ethynyl-linked molecule **6** in comparison with ethenyl-linked molecule **4** (compare Tables IV and V). The oscillator strength increases from 2.01 to 2.22. At the same time, the calculation does not predict any significant shift in the vertical transition energy (in fact, a very small redshift is observed[7]). The Soret band in molecule **6** is represented mainly by the single-electron excitation (214→217) and MO 217 includes porphyrin with a stilbene fragment [Fig. 6(c)]. Both MOs 214 and 217 are antibonding with respect to the two chromophores since they change sign between the porphyrin mesoatom and the triple-bond link. Thus, the Soret band corresponds to excitation of the whole conjugated system which embraces the porphyrin and the ethynyl-linked stilbene moiety. A small CT contribution from the diphenylamine part is also present. Comparison of the ethynyl-linked DPAS and BDPAS (molecules **6** and **7**, respectively) indicates that further redshift occurs for the Q_x band. Our DFT calculation predicts the redshift equal to 10.2 nm, which is very close to the experimental value (10 nm). A similar shift characterizes the *X* band, but its intensity fall down in our DFT prediction. The oscillator strength in molecule **6** decreases from 0.98 to 0.72 in molecule **7**.

We can see from the tables that one-photon absorption spectra in this series of substituted porphyrins undergo systematic changes concerning the nature of the first band and the intensity of the Soret band when going from the parent molecule **1** and single-bond-linked species **2** and **3** to the double-bond-linked molecules **4** and **5**. This is in qualitative agreement with experimental data.[7] The trend is enhanced on going to the triple-bond-linked species **6** and **7**. Although we have not obtained an absolute agreement in calculated transition energies, the trends are reproduced and our calculations permit us to understand the nature of the photophysical transformations upon substitution.

TABLE V. Electronic absorption spectrum of free-base porphyrin derivative **6**. ΔE is an excitation energy (eV), f is an oscillator strength, and M_a is a projection of the electric dipole transition moment (a.u.) on the a axis. Rotatory strenght (R) of electronic circular dichroism (ECD) in 10^{-10} erg esu cm/G.

State D_{2h}	Main CI contributions	ΔE Calc.	ΔE Expt.[a]	M_a M	M_a a	f Calc.	f Expt.[a]	ECD R
S_1X	0.61(214→215)	1.99	2.05	4.48	x	0.979	≈0.9	26.2
	−0.15(214→216)−0.13(212→215)			−0.03	y			
	−0.21(212→216)			0.02	z			
S_2Q	0.22(214→215)+0.49(214→216)	2.11	1.82	1.67	x	0.145	≈0.3	1.5
	+0.40(212→215)−0.13(213→215)			0.04	y			
	−0.22(213→216)			−0.01	z			
S_3	0.61(213→215)+0.28(212→216)	2.31		0.09	x	0.001	···	0.8
	+0.11(214→215)−0.13(214→216)			−0.01	y			
				−0.04	z			
S_4	0.5(213→216)−0.25(212→215)	2.50	2.36	−0.28	x	0.022	≈0.05	0.6
	+0.41(214→216)			0.51	y			
				−0.16	z			
S_5B	0.53(214→217)	2.83	2.82	−5.65	x	2.218	≈2.3	82.7
	+0.14(213→215)−0.34(212→216)			0.01	y			
	+0.16(211→215)			0.00	z			
S_6	0.58(211→215)−0.31(214→217)	2.99		−0.44	x	0.015	···	−5.3
	−0.14(212→216)+0.13(213→215)			0.02	y			
				−0.07	z			

[a]Reference 7.

E. Chirality

We have also calculated electronic circular dichroism (ECD) for all excited states. In Tables II–V, we have presented the calculated optical rotatory strength[47] (ORS) in cgs units (10^{-40} erg esu cm/G). These ECD parameters are calculated in the velocity formulation (the length formulation provides very similar results).

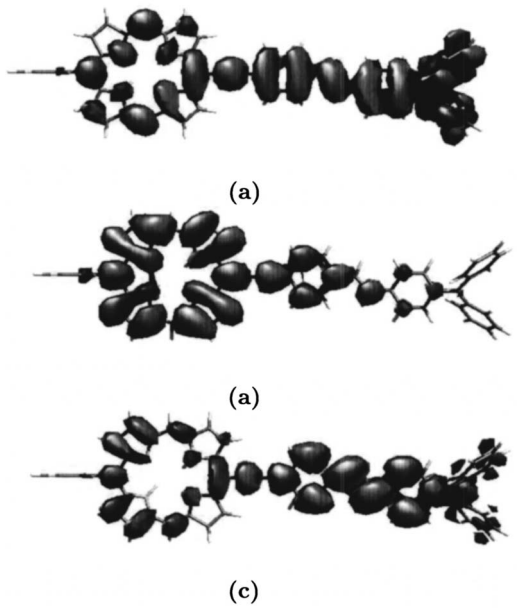

FIG. 6. (a) HOMO (214) of molecule **6**. (b) LUMO (215) of molecule **6**. (c) MO 217 of molecule **6**.

The chiral character of the studied molecules is well manifested in calculated electronic circular dichroism ORS parameters and provides additional characteristics for assignments of the orbital nature of the excited states. In the H_2P molecule, the ORS parameters are equal to zero because of inversion symmetry. Small chirality occurs for the parent molecule **1** (Table II). An addition of (diphenylamino)stilbene group in molecule **2** provides a huge increase of the calculated optical rotatory strength to 91.6 cgs units for the Soret band (Table III). The new intense band in the Q region which occurs starting with the double-bond-linked molecule **4** has also a large ORS parameter (−20.3 cgs units). Its sign is opposite to ORS for the main component of the Soret band. The OSR depends both on the electric (M) and magnetic (μ) dipole transition moments. All transitions with large electronic circular dichroism have big μ components along the y and z axes. Thus, even a small deviation from x polarization for the electric dipole transitions are important for the ECD parameters. Experimental studies of the electronic circular dichroism seem to be very useful for the final assignment of these spectra.

IV. TWO-PHOTON ABSORPTION CROSS SECTIONS

The two-photon absorption spectra of the porphyrin derivatives **1**, **2**, and **4–7** have been recently measured experimentally and reported by Drobizhev *et al.*[7] In Tables VI and VII, we present the calculated two-photon absorption cross sections (σ_{2PA}) for strongly conjugated porphyrin derivatives from **4–7** corresponding to the six lowest states using B3LYP and CAMB3LYP functionals, respectively. The 2PA cross

TABLE VI. Calculated two-photon absorption peak cross sections (σ_{2PA}) at B3LYP/6-31G* of porphyrin derivatives with corresponding laser excitation wavelengths (λ_{ex}) for six lowest state (λ is in nm), σ_{2PA} in the units of GM; Göppert–Mayer=10^{-50} cm^4 s/photon).

	4		**5**		**6**		**7**	
State	λ_{ex}	σ_{2PA}	λ_{ex}	σ_{2PA}	λ_{ex}	σ_{2PA}	λ_{ex}	σ_{2PA}
$S_1(X)$	1210	296.8	1240	488.2	1246	504.9	1272	564.3
$S_2(Q_x)$	1159	268.4	1175	89.2	1175	219.0	1197	129.5
S_3	1060	1201.9	1092	425.3	1073	1533.2	1112	425.6
S_4	992	35.7	1042	1.5	988	13.8	1037	6.8
$S_5(B)$	876	686.9	961	154.2	876	847.8	965	288.2
S_6	826	14.6	898	3.6	829	57.6	895	6.0

sections corresponding to porphyrin derivatives **1** and **2** has not been reported in the table as they are very insignificant compared to molecules **4–7**. From our calculations, it is clear that the 2PA cross section for molecule **1** is predicted to be negligible in agreement with Fig. 2 of Ref. 7 where no measurable 2PA cross section for molecule **1** is seen below 400 nm. A σ_{2PA} value of about 0.1 GM (1 GM $=10^{-50}$ cm^4 s/photon) is detected in this region which corresponds to the Soret band in our calculation in a good agreement with our 2PA cross sections (Table VI). The largest detected σ_{2PA} value at 350 nm for molecule **1** (about 10 GM) is one to two orders of magnitude smaller than the 2PA cross section for other molecules (we did not reach this region with our six-state model for molecule **1**).

The measured σ_{2PA} values corresponding to the Soret region (about 450 nm$\times 2=$900 nm) in molecules **2**, **4**, **5**, and **7** are equal to 100, 560, 880, and 1100 GM, respectively.[7] The calculated results of Table VI provide similar increase in a semiqualitative manner, though the quantitative agreement is not good. Experimentally reported σ_{2PA} values with corresponding laser excitation wavelengths[7] are collected in Table VIII. Making direct comparison of theoretical (Tables VI and VII) and experimental (Table VII) results, we are in a rather awkward situation that there is a rather limited agreement between the calculated vertical transition energies (Tables I–V) and the observed maxima of the 1PA bands, which to some extent can be ascribed to the neglect of Fanck–Condon factors and vibronic perturbations. The discrepancies are enhanced when we consider 2PA spectra. It is here relevant to point out that, for heavily delocalized systems, commonly used functionals show inappropriate asymptotic dependences of excitation energies[55] and polarizabilities,[67,68] and that pure and hybrid DFT functionals may provide poor results for large compounds due to "overpolarization." One should keep in mind that the treatment of charge-transfer excitations is also of concern using local density functionals. We indeed find strong general enhancement of the 2PA cross sections, see Table VI.

Thus, asymptotically corrected functionals, such as CAMB3LYP, show 2PA and 3PA cross section values that in general are much smaller than LDA/B3LYP (but considerably larger than Hartree–Fock),[69,70] which is quite consistent with the observation made in the present calculations (see Table VII). If we compare our calculation based on B3LYP (see Table VI) versus CAMB3LYP (see Table VII), then we observe that all excitation wavelengths have been lowered in case of CAMB3LYP. Another point to note is that all 2PA cross sections are quite sensitive to the excitation wavelength. No doubt, by using CAMB3LYP functional, one can think of capturing the correct ordering of the charge-transfer states but the other states are energetically suppressed. In Ref. 7, the 2PA cross sections are interpreted in terms of the two- or three-level models, while our calculations comprise a many-state approximation and an analysis of the quantum interference contributions (as it was done for the three-level model[7]) is practically impossible. Finally, we have found some discrepancies in the presentation of experimental data in Fig. 2 and Table 1 of Ref. 7. Anyway, scrutinizing the results of highly time-consuming 2PA calculations, some useful trends could be extracted. Before we start our discussion regarding the 2PA cross sections, it is worthwhile to note that none of these molecules have a center of inversion, and, hence, the 2PA transitions could coincide with the 1PA transitions in the corresponding wavelength domain. How-

TABLE VII. Calculated two-photon absorption peak cross sections (σ_{2PA}) of porphyrin derivatives at CAMB3LYP/6-31G* with corresponding laser excitation wavelengths (λ_{ex}) for six lowest state (λ is in nm, σ_{2PA} in the units of GM; Göppert–Mayer=10^{-50} cm^4 s/photon).

	4		**5**		**6**		**7**	
State	λ_{ex}	σ_{2PA}	λ_{ex}	σ_{2PA}	λ_{ex}	σ_{2PA}	λ_{ex}	σ_{2PA}
$S_1(X)$	1198	0.8	1192	1.6	1210	3.3	1212	4.4
$S_2(Q_x)$	1097	3.2	1092	3.8	1112	7.4	1117	11.3
S_3	810	282.8	810	414.8	818	416.8	816	551.4
S_4	736	1.3	738	31.9	742	22.5	747	18.0
$S_5(B)$	694	1378	961	66.6	696	2120	709	3.9
S_6	658	530.3	694	1723.9	665	367.2	696	2726.7

TABLE VIII. Experimentally reported two-photon absorption peak cross sections (σ_{2PA}) of porphyrin derivatives with corresponding laser excitation wavelengths (λ_{ex}) in the Q and Soret regions (λ in nm, σ_{2PA} in the units of GM; Göppert–Mayer$=10^{-50}$ cm^4 s/photon).

	4		5		6		7	
State	λ_{ex}	σ_{2PA}	λ_{ex}	σ_{2PA}	λ_{ex}	σ_{2PA}	λ_{ex}	σ_{2PA}
Q_x	1290	8.5	1284	20	1288	19	1280	49
X	1142	64	1149	130	1141	160	1153	250
S_3	914	560	916	880	907	500	915	1100
B	816	480	826	810	820	730	803	910

ever, at the same time, it is expected that the intensity distributions should be different in the two types of transitions. We see that the 2PA spectra basically follow the 1PA spectra, in contradiction with the experimentally reported results.[7] One reason for this (at least for the Q region) is that we have not taken into account vibronic coupling,[7,71] which presents an ardeous task for such big systems. It is known that absorption in the Q_x region consists of the (0,0) and (0,1) bands including a number of vibronically active modes.[37] The typical four-band spectrum in the Q region of pure porphyrin transforms into a two-band spectrum in the DPAS- and BDPAS-containing molecules.[7] As we have shown in the previous section, this is explained by the fact that the MO structure of pure porphyrin is strongly modified by hyperconjugation with the DPAS and BDPAS substituents in molecules **4–7**. Drobizhev *et al.*[7] have shown that each of the Q_x bands in molecule **7** consists of the overlapping (0,0) and (0,1) lines with $\nu_1=460$ cm^{-1}. This vibrational mode is not very active in the 1PA spectrum, but it induces a quite strong perturbation in the 2PA absorption. Such selectivity of vibronic perturbation in 1PA and 2PA spectra is well known for other molecules[7,71] and can be a reason of the shift in the 1PA and 2PA spectra.

We first need to compare the 2PA spectra of the same class of molecules (same kind of conjugation), such as **2** and **3** (single bonded), **4** and **5** (double bonded), and **6** and **7** (triple bonded), where there is only difference in the length of the substituents. The changes in the 2PA spectra inside the same class of molecules are not large and indicate an increase of the 2PA cross section with increase of conjugation.[7] Some differences in the 2PA spectra of molecules **2** and **3**, where the strongest 2PA cross section is predicted for the X band (but not for the Soret band) in the latter molecule (Table VI) is in agreement with the spectra presented in Fig. 2 of Ref. 7.

A strong increase of the Q-band intensity in the 1PA spectra of molecule **2** in comparison with the simple derivative **1** is explained by effective conjugation between H_2P and the stilbene moiety expressed in the HOMO-LUMO picture (Fig. 4). Both Q bands in molecule **2** include the HOMO $\rightarrow$LUMO excitation (Table III), which represents a large portion of charge transfer from DPAS to porphyrin (Fig. 4). This CT contribution determines an increase of 2PA cross section in comparison with molecule **1**. The authors of Ref. 7 stressed that the absolute σ_{2PA} values of all molecules **2–7** in the lowest Q band are much higher than those obtained earlier for different symmetrically substituted porphyrins; our calculations (Table VI) support this finding and make obvious the increased role of the CT character.

All molecules **2–7** have a strong increase of 2PA cross section in the region of the Soret absorption.[7] The 2PA spectra in the Soret region are quite distinct from the 1PA spectra; while the experimental 1PA Soret absorption consists of one broad band, the 2PA spectra show at least two spectrally resolved peaks.[7] We can explain these 2PA spectra by appearance of the former "gerade" states (in addition to intense 2PA Soret band, Tables III–VI, molecules **4–7**), which are weak and almost invisible in the 1PA transitions, but gets very strong in 2PA. This is the S_3 state in our calculations (Tables III–VI). The 1PA transition to this state has rather small oscillator strength (about 0.01), but the 2PA cross section is predicted to be high (333 GM for molecule **2**, for example). This intense 2PA is shifted to the red from the Soret band (Table VI) in a good agreement with observations.[7] Though this 2PA cross section is overestimated (compare Table VI and Table VIII), an anomalous high intensity of the new 2PA shifted to lower frequency from the Soret band is supported qualitatively by our calculations.

There are two close-lying former "gerade" states, S_3 and S_4 (Tables III–VI), which correspond to the $^1B_{1g}$ and $2\,^1A_g$ states of the parent H_2P molecule (Table I). They are of $\pi\pi^*$ nature in planar porphyrin, but in the nonplanar molecules **2–7**, these states are slightly mixed with $\sigma\pi^*$ excitations in the substituents. Only the S_3 state is very active in the 2PA spectrum; it also contains a large contribution from the HOMO$\rightarrow$LUMO excitation (Tables III–V) in contrast to the S_4 state. The calculated 2PA cross section for the transition to the S_3 state is the largest for the molecules **4** and **6**, in agreement with Fig. 2 of Ref. 7 (this is in a strange contradiction with Table II, taken also from Ref. 7). The state S_3 contains the largest contribution from the HOMO$-1\rightarrow$LUMO excitation in molecules **2** and **6**; the HOMO-1 is localized in the porphyrin ring, thus this transition includes the porphyrin excitation with admixture of charge transfer from the H_2P moiety to the nearest phenyl ring of the DPAS substituent. In molecule **4**, this is the HOMO$-2\rightarrow$LUMO transition with similar nature (Tables III–V, Figs. 4–6).

Strong two-photon absorption at the intrinsic Soret band frequency is determined by the modified nature of the Soret transition in molecules **2–7** (Tables III and VI). As it was discussed before, considering molecule **4** as an example, the shift of the S_5 (B) state with respect to the H_2P molecule is determined by a strong deformation of its wave function; the

main configuration 215→218 (Table IV, Fig. 5) represents simultaneous excitation of both chromophores. In the series of **4**–**7** molecules, these chromophores become more and more coplanar which leads to an increase of hyperconjugation and optical activity of the *B* state.

Finally, we have to discuss an interesting manifestation of the *X* band [$Q_x^{(2)}$ in Ref. 7] in the 2PA spectra. We have to remind that the results of our calculations for the first *X* band (Tables IV–VI, molecules **4–7**) corresponds to the second band in the experimental spectra. The measured σ_{2PA} values increase for the *X* band along the series (64, 130, 160, and 250 GM, respectively);[7] our calculations provide σ_{2PA} values which are about an order of magnitude higher (822, 1352, 1398, and 1563 GM, respectively). We have to remind that the 1PA intensity is also overestimated for the *X* band. This transition consists mostly of the HOMO→LUMO excitation (Tables IV and V). As follows from Figs. 5 and 6, this corresponds to simultaneous excitation of both chromophores with significant CT admixture. Large optical rotatory strength for electronic circular dichroism of this transition (Tables IV and V) is another important feature of the *X* band.

V. CONCLUSIONS

In the framework of linear and quadratic response theory and time-dependent density functional theory (TD DFT), calculations have been applied for a new class of asymmetrical porphyrins with 4-(diphenylamino) stilbene (DPAS) or 4,4′-bis-(diphenylamino) stilbene (BDPAS) as substituents at the mesoposition, being opposite to the dichlorophenyl (DCP) ring, in an attempt to interpret their vertical one-photon (1PA) and two-photon absorption (2PA) spectra. In spite of the fact that two-photon cross sections are overestimated in our TD DFT calculations in comparison with the experimental data of Drobizhev *et al.*,[7] some useful qualitative correlations are obtained.

First, we have shown that the DPAS and BDPAS substituents get more and more coplanar with the porphyrin ring depending on the double-bond and triple-bond links, while the DCP plane is kept orthogonal for all molecules. The corresponding increase in conjugation between the two chromophores provides systematic frequency shifts and intensity redistributions in the observed 1PA and 2PA spectra.[7] A new relatively intense *X* band occurs in the one-photon absorption near 600 nm [denoted as $Q_x^{(2)}$ in Ref. 7]. This is mostly a HOMO→LUMO transition, which includes simultaneous excitation of both chromophores with significant contribution of charge transfer from the substituent to the porphyrin ring.

The charge-transfer character is present in all calculated excited states; its contribution to the Soret band is also appreciable. This includes a simultaneous excitation of both chromophores with a high weight of the substituent. Because of this reason, the 1PA Soret band is strongly enhanced and broadened and exhibits also a strong 2PA cross section.

A hidden transition to the "gerade" state of the parent porphyrin is shifted to lower frequencies from the Soret band and becomes very active in the 2PA spectrum; it has the main contribution from the HOMO−2→LUMO transition in molecules **4–6** and includes a predominant excitation inside the porphyrin ring with essential charge-transfer character. Thus, an intense two-photon absorption corresponding to the Soret region occurs at about 2×460 nm=920 nm (the former "gerade" state S_3) and at about 2×410 nm=820 nm (the Soret state). These two 2PA bands are induced by charge-transfer contributions.

It has been shown in this study that the new asymmetric DPAS or BDPAS substituents at the mesoposition in the porphyrin ring could lead to a drastic change in the 2PA cross section depending upon the nature of the π-conjugated linkers. At least two rather strong 2PA transitions in the near IR range have been found for the double-bond and triple-bond linkers in a semiqualitative agreement with experiment. Calculations predict an increasing 2PA cross section corresponding to Q_x and *X* bands (about 1300–1200 nm) with increase of π conjugation in this class of molecules.

As a result of this study, it is clear how the combination of linkers with a particular kind of substituent at a particular position leads to salient changes in the 2PA cross sections. This exemplifies the possibilities to use unique molecular features in the design of chromophores with strong 2PA for use in photodynamic therapy and biological imaging.

ACKNOWLEDGMENTS

The authors acknowledge a grant from the photonics project run jointly by the Swedish Materiel Administration (FMV) and the Swedish Defense Research Agency (FOI). This work has also been supported by the Swedish Research Council. One of the author (P.C.J.) would specially like to thank Wenner-Gren Foundation for postdoctoral grant.

[1] G. P. Gurinovich, A. N. Sevchenko, and K. N. Solovjev, *Spectroscopy of Chlorophyll and Related Compounds* (Science and Technology, Minsk, 1968).
[2] A. J. Hoff and J. Deisenhofer, Phys. Rep. **287**, 1 (1997).
[3] N. Z. Mamardashvili and O. A. Golubchikov, Russ. Chem. Rev. **70**, 577 (2001).
[4] M. Gouterman, *The Porphyrins*, edited by D. Dolphin (Academic, New York, 1978), Vol. III, p. 1.
[5] L. L. Gladkov, A. T. Gradyushko, A. M. Shulga, K. N. Solovyov, and A. Starukhin, J. Mol. Struct.: THEOCHEM **45**, 463 (1978).
[6] L. A. Bykovskaya, A. T. Gradyushko, R. I. Personov, Yu. V. Romanovskij, K. N. Solovyov, A. M. Shulga, and A. Starukhin, Izv. Akad. Nauk SSSR, Ser. Fiz. **44**, 822 (1980).
[7] M. Drobizhev, F. Meng, A. Rebane, Y. Stepanenko, E. Nickel, and C. W. Spangler, J. Phys. Chem. B **110**, 9802 (2006).
[8] A. R. Battersby, C. J. R. Fookes, G. W. J. Matcham, and E. McDonald, Nature (London) **285**, 559 (1980).
[9] B. Felber and F. Diederich, Helv. Chim. Acta **88**, 120 (2005).
[10] R. Vestberg, A. Nystrom, M. Lindgren, E. Malmstrom, and A. Hult, Chem. Mater. **16**, 2794 (2004).
[11] M. Drobizhev, Y. Stepanenko, Y. Dzenis, A. Karotki, A. Rebane, P. N. Taylor, and H. L. Anderson, J. Phys. Chem. **109**, 7223 (2005).
[12] M. Kruk, A. Karotki, M. Drobizhev, V. Kuzmitsky, V. Gael, and A. Rebane, J. Lumin. **105**, 43 (2003).
[13] M. A. Baldo, D. F. O'Brien, M. E. Thompson, and S. R. Forrest, Phys. Rev. B **60**, 14422 (1999).
[14] M. A. Baldo and S. R. Forrest, Phys. Rev. B **62**, 10958 (2000).
[15] J. S. Wilson, A. S. Dhoot, A. J. Seeley, M. S. Khan, A. Kohler, and R. H. Friend, Nature (London) **413**, 828 (2001).
[16] Y. Y. Noh, C. L. Lee, J. J. Kim, and K. Yas, J. Chem. Phys. **118**, 2853 (2003).

[17] J. E. Rogers, K. A. Nguyen, D. C. Hufnagle, D. G. McLean, W. Su, K. M. Gossett, A. R. Burke, S. A. Vinogradov, R. Pachter, and P. A. Fleitz, J. Phys. Chem. A **107**, 11331 (2003).
[18] R. A. Oakes and S. E. J. Bell, J. Phys. Chem. A **107**, 2964 (2003).
[19] A. A. Jarzecki, P. M. Kozlowski, P. Pulay, B. H. Ye, and X. Y. Li, Spectrochim. Acta, Part A **53**, 1195 (1997).
[20] H. Nakatsuji, J. Hasegawa, and M. Hada, J. Chem. Phys. **104**, 2321 (1996).
[21] K. Ohkawa, M. Hada, and H. Nakatsuji, J. Porphyr. Phthalocyanines **5**, 256 (2001).
[22] D. Sundholm, Phys. Chem. Chem. Phys. **2**, 2275 (2000).
[23] K. A. Nguyen, P. N. Day, and R. Pachter, J. Phys. Chem. A **104**, 4748 (2000).
[24] K. A. Nguyen and R. Pachter, J. Chem. Phys. **118**, 5802 (2003).
[25] L. Edwards, D. H. Dolphin, M. Gouterman, and A. D. Adler, J. Mol. Spectrosc. **38**, 16 (1971).
[26] M. P. Tsvirko, K. N. Solovjev, A. T. Gradyushko, and S. S. Dvornikov, Zh. Prikl. Spektrosk. **20**, 528 (1974).
[27] A. T. Gradyushko, K. N. Solovyov, A. M. Shulga, and A. Starukhin, Opt. Spectrosc. **43**, 37 (1977).
[28] J. G. Radziszewski, J. Waluk, M. Nepras, and J. Michl, J. Phys. Chem. **95**, 1963 (1991).
[29] B. M. Kharlamov, L. A. Bykovskaya, and R. I. Personov, Chem. Phys. Lett. **50**, 407 (1977).
[30] S. Tobita, Y. Kaizu, H. Kobayashi, and I. Tanaka, J. Chem. Phys. **81**, 3568 (1984).
[31] M. Gouterman, J. Mol. Spectrosc. **6**, 138 (1961).
[32] J. D. Baker and M. C. Zerner, Chem. Phys. Lett. **175**, 192 (1990).
[33] R. Bauernschmitt and R. Ahlrichs, Chem. Phys. Lett. **256**, 454 (1996).
[34] S. J. A. van Gisbergen, A. Rosa, G. Ricciardi, and E. J. Baerends, J. Chem. Phys. **111**, 2499 (1999).
[35] O. Loboda, I. Tunnell, B. F. Minaev, and H. Ågren, Chem. Phys. **312**, 299 (2005).
[36] B. F. Minaev and H. Ågren, Chem. Phys. **315**, 215 (2005).
[37] B. Minaev, Y.-H. Wang, C.-K. Wang, Y. Luo, and H. Ågren, Spectrochim. Acta, Part A **65**, 308 (2006).
[38] M. Kleischmidt, J. Tatchen, and C. M. Marian, J. Chem. Phys. **124**, 124101 (2006).
[39] B. F. Kim and J. Bohandy, J. Mol. Spectrosc. **73**, 332 (1978).
[40] W. Kohn and L. J. Sham, Phys. Rev. Lett. **52**, 997 (1984).
[41] A. D. Becke, J. Chem. Phys. **98**, 5648 (1993).
[42] K. A. Nguyen, P. N. Day, and R. Pachter, J. Chem. Phys. **110**, 9135 (1999).
[43] J. Hasegawa, Y. Ozeki, M. Hada, and H. Nakatsuji, J. Phys. Chem. B **102**, 1320 (1998).
[44] M. H. Perrin, M. Gouterman, and C. L. Perrin, J. Chem. Phys. **50**, 4137 (1969).
[45] W. J. Hehre, R. Ditchfield, and J. A. Pople, J. Chem. Phys. **56**, 2257 (1972).
[46] K. D. Dobbs and W. J. Hehre, J. Comput. Chem. **8**, 880 (1987).
[47] M. J. Frisch, G. W. Trucks, H. B. Schlegel, *et al.*, GAUSSIAN 03, Revision B05, Gaussian, Inc., Pittsburgh, PA, 2003.
[48] J. Autschbach, T. Ziegler, S. J. A. van Gisbergen, and A. J. Baerends, J. Chem. Phys. **116**, 6930 (2002).
[49] W. M. McClain, J. Chem. Phys. **55**, 2789 (1971); **57**, 2264 (1972).
[50] T. Kogej, D. Beljonne, F. Meyers, J. W. Perry, S. R. Marder, and J. L. Bredas, Chem. Phys. Lett. **298**, 1 (1996).
[51] M. Albota, D. Beljonne, J. L. Brdas, J. E. Ehrlich, J. Y. Fu, A. A. Heikal, S. E. Hess, T. Kogej, M. D. Levin, S. R. Marder, D. McCord–Maughon, J. W. Perry, H. Rckel, M. Rumi, G. Subramaniam, W. W. Webb, X. Wu, and C. Xu, Science **281**, 1653 (1998).
[52] P. Norman, Y. Luo, and H. Ågren, J. Chem. Phys. **111**, 7758 (1999).
[53] M. B. Masthay, L. A. Findsen, B. M. Pierce, D. F. Bocian, J. S. Lindsey, and R. R. Birge, J. Chem. Phys. **84**, 3901 (1985).
[54] M. J. G. Peach, T. Helgaker, P. Sałek, T. W. Keal, O. B. Lutnæs, D. J. Tozer, and N. C. Handy, Phys. Chem. Chem. Phys. **8**, 558 (2006).
[55] Z. L. Cai, K. Sendt, and J. R. Reimers, J. Chem. Phys. **117**, 5543 (2002).
[56] Z. L. Cai, M. J. Crossley, J. R. Reimers, R. Kobayashi, and R. D. Amos, J. Phys. Chem. B **110**, 15624 (2006).
[57] S. Grimme and M. Parac, ChemPhysChem **4**, 292 (2003).
[58] T. Yanai, D. P. Tew, and N. C. Handy, Chem. Phys. Lett. **393**, 51 (2004).
[59] M. J. Paterson, O. Christiansen, F. Pawlowski, P. Jorgensen, C. Hattig, T. Helgaker, and P. Salek, J. Chem. Phys. **124**, 054322 (2006).
[60] J. Arnbjerg, A. Jimenez–Banzo, M. J. Paterson, S. Nonell, J. I. Borrell, O. Christiansen, and P. R. Ogilby, J. Am. Chem. Soc. **129**, 5188 (2007).
[61] DALTON, Release 2.0, a molecular electronic structure program, 2005, see http://www.kjemi.uio.no/software/dalton/dalton.html
[62] L. Serrano–Andres, M. Merchan, M. Rubio, and B. O. Roos, Chem. Phys. Lett. **295**, 195 (1998).
[63] Y. Tokita, J. Hasegawa, and H. Nakasuji, J. Phys. Chem. A **102**, 1843 (1998).
[64] T. Hashimoto, Y.-K. Choe, H. Nakano, and K. Hirao, J. Phys. Chem. A **103**, 1894 (1999).
[65] X.-Y. Li and M. Z. Zgierski, J. Phys. Chem. **95**, 4268 (1991).
[66] M. Lindgren, B. Minaev, E. Glimsdal, R. Vestberg, R. Westlund, and E. Malmstrom, J. Lumin. **124**, 302 (2007).
[67] B. Champagne, E. A. Perpète, S. J. A. van Gisbergen, E. J. Baerends, J. G. Snijders, C. Soubra–Ghaoui, K. A. Robins, and B. Kirtman, J. Chem. Phys. **109**, 10489 (1998).
[68] B. Champagne, E. A. Perpète, D. Jacquemin, S. J. A. van Gisbergen, E. J. Baerends, C. Soubra–Ghaoui, K. A. Robins, and B. Kirtman, J. Phys. Chem. A **104**, 4755 (2000).
[69] E. Rudberg, P. Sałek, T. Helgaker, and H. Ågren, J. Chem. Phys. **123**, 184108 (2005).
[70] P. Sałek, H. Ågren, A. Baev, and P. N. Prasad, J. Phys. Chem. A **109**, 11037 (2005).
[71] Y. Luo, H. Ågren, S. Knut, B. Minaev, and P. Jrgensen, Chem. Phys. Lett. **209**, 513 (1993).